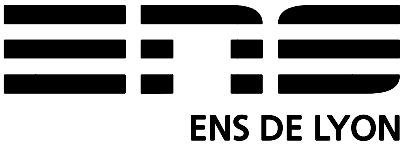

Master Science de la matière
École Normale Supérieure de Lyon

Internship 2020–2021
Antoine Sérandour
M1 Physics

Determining the size of an electron beam using a Beam Position Monitor

Abstract : *Beam Position Monitors (BPMs) are commonly used in particles accelerators to determine the position of a beam. The device is however sensible to other parameters of the beam, especially the diameter. If the electronic noise can blur this sensitivity, several measurements can statistically reveal the dependency on the diameter. This study proposes such a statistical treatment with the resolution expected for the accelerator ThomX. This study calls for further investigations, especially experimental developments, to confirm the feasibility and the efficiency of this treatment to determine the shape of the ring lattice in ThomX.*

Key words : *BPM, particles accelerator, electronic noise*

Internship supervised by :
DELERUE Nicolas
delerue@lal.in2p3.fr / phone (+33) 1 64 46 84 66
Laboratoire de Physique des 2 infinis Irène Joliot-Curie – IJCLab
15 rue Georges Clémenceau
91405 ORSAY CEDEX
https://www.ijclab.in2p3.fr/

May 30, 2024

Remerciements

Je souhaiterais remercier toute l'équipe de l'IJClab, en particulier Nicolas Delerue qui s'est toujours montré très à l'écoute. Je le félicite encore pour l'heureux évènement et lui souhaite bonne continuation ! Je tiens également à remercier Alexandre Moutardier et Emmanuel Goutierre pour leur aide et les multiples discussions physiques qui parfois partaient trop loin, il faut le dire ! Bonne chance pour vos thèses respectives ! Enfin, je voulais remercier mes camarades Partheepan Senthilnathan et Honorin Portela avec qui partager des repas était un vrai régal, parfois meilleur que les plats du RU. Merci à tous et bonne continuation !

Contents

Introduction

Particles accelerators have a wide range of applications, both in fundamental fields such as High Energy Physics or Nuclear Physics and in applied fields such as cancer treatment and food sterilization. This report will account for an internship at the IJClab, where an accelerator called ThomX is under construction. This project aims at producing a beam of electrons at 50 MeV that will be used in the production of X-rays. The first beam is planned for the end of the year 2021.

To study the phenomena happening in an accelerator, the experiment includes many measuring instruments placed at several places on the electrons path. The aim of this internship is to use one of these instruments called BPM (Beam Positioning Monitor) in the determination of one characteristic quantity of the beam in the accelerator, its diameter. A BPM is composed of four electrodes that are commonly used in order to provide the position of the beam inside them. This internship will study the sensitivity of this device to the diameter of the beam in order to extract this information from the signals of the BPM.

This subject has been studied since 1983 with the work of Miller [1], which propose a method to measure the difference between the x and the y transverse length of a beam, using a set of several measurements of the same beam in a BPM. Further investigations were made to propose a method with movable BPMs to measure with more accuracy [2]. All these works provide the difference between the x and y transverse lengths of the beam, but no one could provide directly the value of those transverse lengths. The aim of this study is to find a method giving the order of magnitude of the transverse length.

This report will first account for a determination of the electric field applied by a beam on one electrode of a BPM, then it will expose an analytical resolution to extract the position and the diameter from this field, before studying the impact of the noise on this resolution. Finally a statistical treatment will be introduce to decrease the noise impact.

1 Signal on the electrodes of a BPM

1.1 Theoretical signal of a beam on an electrode

The electric field applied by a beam made of electrons on the electrodes of a BPM can be calculated. Let's consider a beam uniformly charged and with a total charge Q. This beam has a circular section with a diameter d, and its center is located at the coordinates (x, y) relative to the center of the BPM, as shown in the figure 1. In a first approximation, one can suppose the beam has the shape of a cylinder infinitely long. The beam is composed of infinitely thin fibers. The electric field caused by one of these

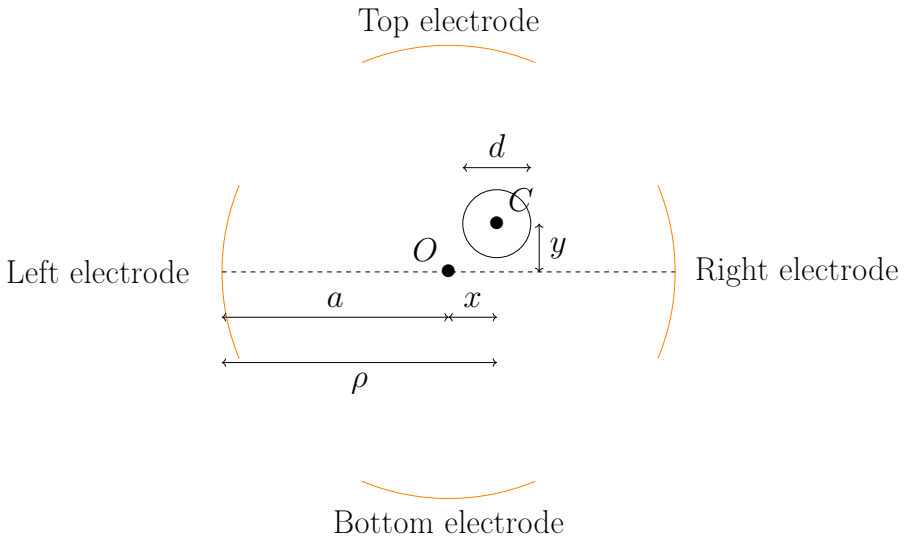

Figure 1: Diagram representing a BPM with its four electrodes in orange, and inside it the beam of center C at the coordinate (x, y) with a diameter d. The distance $a + x$ is written ρ as it will be an important distance in the following.

fibers E_{fiber} is given by Maxwell-Gauss equation that one integrates on a cylindrical volume $\mathcal{V}$ with a surface $\mathcal{S}$, as shown in figure 2.

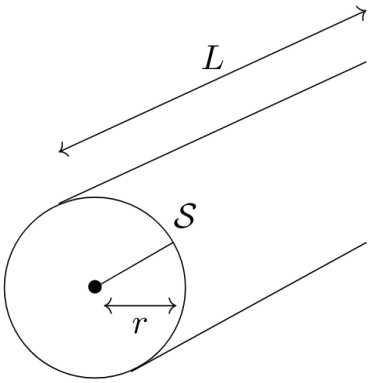

Figure 2: Diagram representing the surface on which the electric field is constant for an infinitely thin fiber of a beam. r is the radius of the cylinder and L is its the length.

$$\operatorname{div} \mathbf{E}_{\text{fiber}} = \frac{\rho}{\epsilon_0}, \tag{1}$$

$$\int_{\mathcal{V}} \operatorname{div} \mathbf{E}_{\text{fiber}} \, \mathrm{d}\tau = \int_{\mathcal{V}} \frac{\rho}{\epsilon_0} \, \mathrm{d}\tau, \tag{2}$$

$$\int_{\mathcal{S}} \mathbf{E}_{\text{fiber}}.\mathrm{d}\mathbf{S} = \frac{q}{\epsilon_0}, \tag{3}$$

$$E_{\text{fiber}}(r) 2\pi r L = \frac{q}{\epsilon_0}, \tag{4}$$

$$\mathbf{E}_{\text{fiber}}(r, \theta, z) = \frac{q}{2\pi L \epsilon_0} \frac{1}{r} \mathbf{u}_r, \tag{5}$$

with ρ the charge density, L the length of the cylinder, q the charge of the beam inside the cylinder and (r, θ, z) the cylindrical coordinates. One can note that the electric field is constant on the cylinder.

Electrodes in a BPM are curved metal plates with a radius of curvature a, which corresponds to the distance between the electrode and the center of the BPM (for more information on BPMs, see [3]). The calculations can be reduced to the case of one electrode, for example the left one. The surface of the cylinder has a radius of curvature close to the one of the electrode : $a \simeq \sqrt{(a+\xi)^2 + \upsilon^2}$ with (ξ, υ) the coordinates of the fiber relative to the center of the BPM. Another approximation will be made supposing that the two surfaces overlap. Hence, the electric field caused by a fiber is uniform in the electrode and is $\frac{q}{2\pi L \epsilon_0} \frac{1}{r}$ with $r = \sqrt{(a+\xi)^2 + \upsilon^2}$.

Finally, in order to simplify the calculation, one can suppose that $\upsilon^2 \ll a^2$. The electric field can be written as :

$$E_{\text{fiber}} = \frac{q}{2\pi L \epsilon_0} \frac{1}{a+\xi}. \tag{6}$$

Let's consider that the fibers are infinitesimal with a charge $\mathrm{d}q = \frac{\tilde{Q}}{\pi (d/2)^2} \mathrm{d}S$, since the fiber are uniformly distributed. $\tilde{Q}$ corresponds to the charge inside the cylinder. The electric field caused $E_{\text{electrode}}$ by the whole beam is given by integrating the E_{fiber} on all the positions of the fibers. $E_{\text{electrode}}$ does not depend on the y since E_{fiber} does not depend on υ, so that the calculation can be made considering that the center of the beam is along the x axis. The schema of the integral is presented in figure 3. The term $a + x = \rho$ appears and represents the distance between the electrode and the center of the beam.

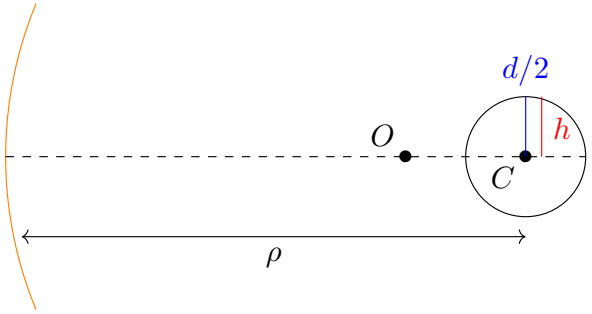

Figure 3: Diagram describing the integration giving $E_{\text{electrode}}$. The integration on υ is constant from $-h$ to h, with h depending on ξ.

$$E_{\text{electrode}} = \int_S E_{\text{fiber}}(r), \tag{7}$$

$$= \int_S \frac{\tilde{Q}}{\pi(d/2)^2} \frac{1}{2\pi L\epsilon_0} \frac{1}{a+\xi}\,\mathrm{d}S, \tag{8}$$

$$= \frac{\tilde{Q}}{\pi(d/2)^2} \frac{1}{2\pi L\epsilon_0} \int_{x-d/2}^{x+d/2} \mathrm{d}\xi \int_{-h}^{h} \mathrm{d}\upsilon\, \frac{1}{a+\xi}, \tag{9}$$

$$= \frac{\tilde{Q}}{2\pi^2 L\epsilon_0 (d/2)^2} \int_{x-d/2}^{x+d/2} \frac{2h(\xi)}{a+\xi}\,\mathrm{d}\xi. \tag{10}$$

One can choose $\xi' = \xi - x$ to simplify the integration.

$$E_{\text{electrode}} = \frac{\tilde{Q}}{\pi^2 L\epsilon_0 (d/2)^2} \int_{-d/2}^{d/2} \frac{\sqrt{(d/2)^2 - \xi'^2}}{\rho + \xi'}\,\mathrm{d}\xi', \tag{11}$$

$$= \frac{\tilde{Q}}{\pi^2 L\epsilon_0 (d/2)^2} \left[-\sqrt{\rho^2 - (d/2)^2} \arcsin\left(\frac{\rho\xi' + (d/2)^2}{d/2(\rho+\xi')}\right) + \rho \arcsin\left(\frac{\xi'}{d/2}\right) + \sqrt{\rho^2 - \xi'^2} \right]_{-d/2}^{+d/2}, \tag{12}$$

$$= \frac{\tilde{Q}}{\pi^2 L\epsilon_0 (d/2)^2} \left(-\sqrt{\rho^2 - (d/2)^2}\pi + \rho\pi \right), \tag{13}$$

$$E_{\text{electrode}} = \frac{\tilde{Q}}{L\pi\epsilon_0} \frac{1}{\eta^2 \rho} \left(1 - \sqrt{1-\eta^2}\right), \tag{14}$$

with $\eta = \frac{d}{2\rho}$, $\rho = a + x$, and $\tilde{Q}$ the charge of the beam inside the cylinder. L is chosen so that the cylinder corresponds to the BPM, so $L = 100$ mm. $\tilde{Q}$ corresponds to the charge inside the BPM, this charge $\tilde{Q}$ is proportional to the total charge Q. We will thus use the same value for Q and $\tilde{Q} \sim 1$ nC.

The expression of the electric field in the other electrodes can be derived from this expression by replacing x by $-x$ for the right electrode, y for the bottom one and $-y$ for the top one.

The equation 14 can be simplified by a Taylor development in η since the diameter is negligible with respect to the diameter of the BPM $2a$. The development gives the following expression :

$$E_{\text{electrode}} \simeq \frac{\tilde{Q}}{2\pi L\epsilon_0} \frac{1 + \eta^2/4}{\rho}. \tag{15}$$

The evolution of the field E with the different variables x, d and Q is represented in the figure 4. The position is measured in x/a to determine the shift from the center, and the diameter is measured in $d/2a$ correspond to the ratio of the diameter of the beam by the one of the BPM. The $d/2a$ ratio will be an important quantity, as it give an order of magnitude of η.

This figure 4 illustrates the effect of the position, the diameter and the charge of the beam on the electric field. First, the electric field is proportional to the charge, as expected by the expression of the field in the equation 14. A difference of 1 mm in position will affect the field for about 10 %, where a difference of 1 mm in diameter will affect the field for about 0.1 %. Thus the field is much less dependant on the diameter than on the position. Indeed, those graphs show that the diameter is the parameter that affects the least the electrical field.

Three hypotheses are needed to obtain the equation 14: the beam is long enough to be considered of infinite length, the cylinder and the electrode overlap, and $\upsilon^2 \ll a^2$.

The last one is validated by the dimension of the BPM and the shape of the beam. Indeed, $a = 20$ mm and $x, y, d \sim 1$ mm.

The electrons are propagating at a speed close to the speed of light c and the length of the beam is about 1 mm (which corresponds to a propagation of 1 ps). The length of the BPM is $L = 100$ mm, so the beam cannot be considered of infinite length. However, the signal measured is not the instantaneous

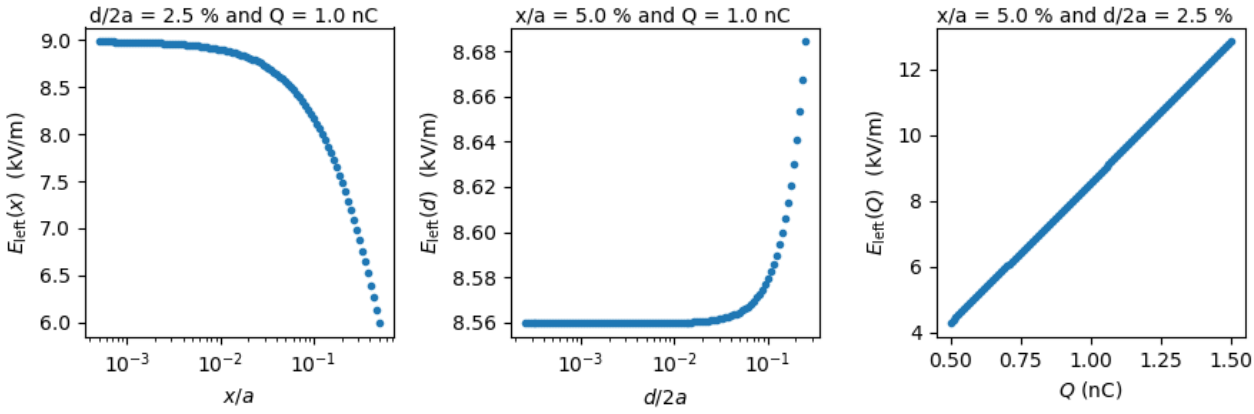

Figure 4: Evolution of the electric field on the left electrode with respect to the parameters of the beam x/a (left), $d/2a$ (middle), and Q (right). A difference of 1 mm in position will affect the field for about 10 %, where a difference of 1 mm in diameter will affect the field for about 0.1 %. The positions and diameters are given with respect to the radius of the BPM a: $d = 1$ mm corresponds to $d/2a = 2.5$ %, and $x = 1$ mm corresponds to $x/a = 5.0$ % (with $a = 20$ mm).

electric field but an integration of this field during a time interval. The sampling frequency of the BPM is around 10 ns, which corresponds to a propagation of 3 m for the beam. The length of the beam integrated is thus much longer than the BPM length and the beam can be considered of infinite length.

The cylindrical Gauss surface and the electrode do not perfectly overlap, which means that the field has not a uniform value on the whole electrode. To verify the overlap hypothesis, it is necessary to determine the maximal variation of the field on an electrode. Let's considers a fiber of the beam M placed in (ξ, υ) with $\xi > 0$ and $\upsilon > 0$, as shown in figure 5. The maximum value of the field is obtained for the nearest point of the electrode, the minimum value on the farthest. The electrode is curved with a radius a and has an angular opening of $2\alpha \sim 50°$. A point of the electrode is localised with $(a\cos(\phi), a\sin(\phi))$, where ϕ is the angle formed by its radius and the x axis. The distance between the fiber and the electrode can be determined, as well as its derivative :

$$r(\phi) = \sqrt{(\xi - a\cos(\phi))^2 + (\upsilon - a\cos(\phi))^2}, \tag{16}$$

$$\frac{\mathrm{d}\, r(\phi)}{\mathrm{d}\phi} = \frac{a}{r(\phi)} \left(\xi \sin(\phi) - \upsilon \cos(\phi)\right). \tag{17}$$

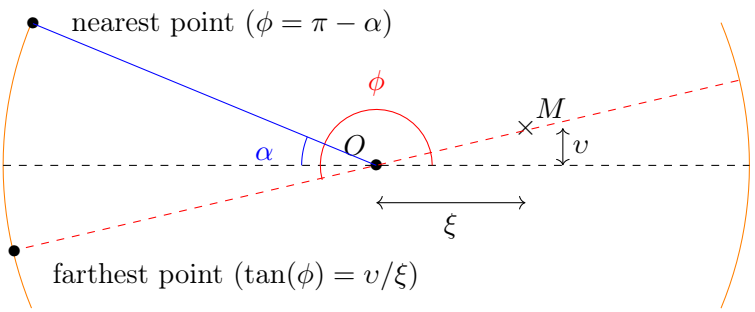

Figure 5: Diagram representing a fiber M of the beam in a BPM. The angle ϕ is given by $\tan\phi = \xi/\upsilon$, which corresponds to the angle of the line passing through the origin O and the fiber M. The point on the left electrode with this angle ϕ corresponds to the maximum of the field.

The extreme fields are localised on the left electrode where $r'(\phi) = 0$ or at the edge of the electrode. Since ξ and υ are positive, the point $(-a\cos(\alpha), a\sin(\alpha))$ (for $\phi = \pi - \alpha$) is always the nearest point. $r'(\phi) = 0$ means $\tan\phi = \xi/\upsilon$, this is possible only if $\frac{\upsilon}{\xi} < \tan(\alpha)$. Therefore, the farthest point is located at ϕ with $\tan\phi = \xi/\upsilon$ (see fig 5), or at the bottom edge of the electrode $\phi = \pi + \alpha$.

$$\delta(\phi) = \frac{E_{\max} - E_{\min}}{E_{\max} + E_{\min}} = \frac{\frac{1}{r(\pi-\alpha)} - \frac{1}{r(\phi)}}{\frac{1}{r(\pi-\alpha)} + \frac{1}{r(\phi)}}, \tag{18}$$

$$= \frac{\sqrt{\frac{(\xi - a\cos(\phi))^2 + (\upsilon - a\sin(\phi))^2}{(\xi - a\cos(\pi-\alpha))^2 + (\upsilon - a\sin(\pi-\alpha))^2}} - 1}{\sqrt{\frac{(\xi - a\cos(\phi))^2 + (\upsilon - a\sin(\phi))^2}{(\xi - a\cos(\pi-\alpha))^2 + (\upsilon - a\sin(\pi-\alpha))^2}} + 1}. \tag{19}$$

The study of the term under the square root will give the highest difference of the fields.

$$\sqrt{\frac{(\xi - a\cos(\phi))^2 + (\upsilon - a\sin(\phi))^2}{(\xi - a\cos(\pi-\alpha))^2 + (\upsilon - a\sin(\pi-\alpha))^2}} = \sqrt{\frac{\xi^2 + \upsilon^2 - 2a(\xi\cos\phi + \upsilon\sin\phi) + a^2}{\xi^2 + \upsilon^2 - 2a(\xi\cos(\pi-\alpha) + \upsilon\sin(\pi-\alpha)) + a^2}}. \tag{20}$$

For $\upsilon/\xi > \tan(\pi+\alpha)$, and therefore $\phi = \pi + \alpha$:

$$\sqrt{\frac{(\xi - a\cos(\phi))^2 + (\upsilon - a\sin(\phi))^2}{(\xi - a\cos(\pi-\alpha))^2 + (\upsilon - a\sin(\pi-\alpha))^2}} = \sqrt{\frac{A - 2a\upsilon\sin(\pi+\alpha)}{A - 2a\upsilon\sin(\pi-\alpha)}}, \tag{21}$$

$$\simeq \sqrt{1 + 4a\upsilon\sin\alpha/A}. \tag{22}$$

with $A = a^2 + \xi^2 + \upsilon^2 - 2a\xi\cos(\pi-\alpha) \sim a^2$. Since $\upsilon \ll a$:

$$\delta(\phi) = \frac{E_{\max} - E_{\min}}{E_{\max} + E_{\min}} \simeq \frac{2a\upsilon\sin\alpha/A}{2 + 2a\upsilon\sin\alpha/A}, \tag{23}$$

$$\sim \frac{\upsilon}{a}\sin\alpha \sim \frac{\upsilon}{a} \times 4.10^{-1} \tag{24}$$

The relative difference δ is low since $\upsilon/a \sim 10^{-2}$.

For $\upsilon/\xi = \tan\phi$:

$$\sqrt{\frac{(\xi - a\cos(\phi))^2 + (\upsilon - a\sin(\phi))^2}{(\xi - a\cos(\pi-\alpha))^2 + (\upsilon - a\sin(\pi-\alpha))^2}} = \sqrt{\frac{B - 2a\xi\cos\phi(1 + \tan^2\phi)}{B - 2a\xi\cos(\pi-\alpha)(1 + \tan\phi\tan(\pi-\alpha))}} \tag{25}$$

$$\simeq \sqrt{1 - \frac{2a\xi}{B}\Big(\cos\phi(1 + \tan^2\phi) + \cos(\alpha)(1 - \tan\alpha\tan\phi)\Big)}. \tag{26}$$

with $B = a^2 + \xi^2 + \upsilon^2 \sim a^2$. Considering $\xi \ll a$:

$$\delta(\phi) \simeq -\frac{\xi}{2a}\Big(\cos\phi(1 + \tan^2\phi) + \cos\alpha(1 - \tan\alpha\tan\phi)\Big), \tag{27}$$

$$= \frac{\xi}{2a} f(\phi, \alpha). \tag{28}$$

The function $f(\phi, \alpha)$ determines the maximum of the difference :

$$\frac{\partial\, f(\phi,\alpha)}{\partial\phi} = -\frac{\sin\phi - \sin\alpha}{\cos^2\phi} > 0 \quad \text{for } \phi \in [\pi, \pi+\alpha]. \tag{29}$$

The derivative is positive since $\sin\phi < 0$, so f increase with ϕ and so does $\delta(\phi)$. The maximum of δ corresponds to $\phi = \pi + \alpha$, which has already been calculated.

$$\delta(\phi) < \frac{\xi}{2a} f(\pi+\alpha, \alpha), \tag{30}$$

$$< \frac{\xi}{2a} 2\cos\alpha\tan^2\alpha, \tag{31}$$

$$< \frac{\upsilon}{a}\cos\alpha\tan\alpha, \tag{32}$$

$$\delta(\phi) < \frac{\upsilon}{a} \times 4\ 10^{-1}. \tag{33}$$

In both cases ($\phi < \pi + \alpha$ or $\phi = \pi + \alpha$), the difference between the electric field maximum and minimum is less than 10 %. The field can be considered uniform on the electrodes.

1.2 Simulation of the beam

An analytical expression 14 of the field on an electrode was obtained in the previous paragraph. However, the analytical expression does not represent exactly the field on the electrode, since some hypotheses were supposed and the beam is made of electrons that create a finite distribution of charge, and not a uniform cylindrical charge. The validity of the hypotheses was exposed in the previous paragraph, and this paragraph will address the question of the statistics. To verify whether there is enough electrons in the beam so that the analytical expression 14 is validated or not, a simulation was performed for a finite number of electrons. This study is also a way to validate the expression of the field 14.

The simulations are made under Python3 using the library numpy. The positions (ξ_i, υ_i) of N_{part} are spread randomly in a circle of radius $d/2$ with an offset so that the center of the circle is in (x, y). These electrons are all in the same plane, which is perpendicular to the beam and in the middle of the BPM.

Let's now determine the field produced by one electron on an electrode. The electron will be considered as an isolated charge. The field produced is uniform on a sphere whereas the electrodes are cylindrical, so the field will not be uniform on the electrode. One can assume that an effective uniform field is applied on the electrode. The expression of this field respects the Gauss theorem :

$$E(r)\mathcal{S}_{\text{sphere}}(r) = \frac{Q_{\text{e}}}{\epsilon_0} = E_{\text{eff}}(r)\mathcal{S}_{\text{cylinder}}(r), \tag{34}$$

$$E_{\text{eff}} = \frac{Q_{\text{e}}}{\epsilon_0}\frac{1}{2\pi r L + \pi r^2}. \tag{35}$$

Since the length L corresponds to the length of the BPM, $r \ll L$, so the effective field is given by the expression :

$$E_{\text{eff}} = \frac{Q_{\text{e}}}{2\pi L \epsilon_0}\frac{1}{r}, \tag{36}$$

where r is the distance between the electron and the electrode in the plane containing the electrons. This expression is very similar to the equation giving the field of a fiber (equation 5). This similarity was expected since the approximation of an effective field is equivalent to *stretching the electrons*. Considering that all the electrons are in the same plane is not a bad approximation since the expression obtained corresponds to stretched electrons. There is however one difference between the two expressions : the charge q in the equation 5 is the charge contained in the BPM whereas the charge Q_{e} is the whole charge of the electron. However, since the BPM will integrate on 3 m a beam of 1 mm long, there is no difference in the end.

The simulation will then sum all the fields applied by the electrons on an electrode and then return the effective total field on each electrode. We recall that the aim is to verify that these fields are diameter dependant, even though there is a finite distribution of charge, and find the number of electron that would be suitable to approximate the distribution with a continuous distribution of charge.

The results of the simulation is given in figure 6. One can note that the simulation converge with the number of electrons, which was expected. The convergence happens for $N_{\text{part}} \sim 10^5$, which means that the analytical expression of $E_{\text{electrode}}$ 14 is valid for more than 10^5 electrons for a beam with $d/2a = 2.5$ %. The beam in ThomX is supposed to have a charge of 1 nC, so the beam is made of a billion of electrons. Therefore, the study will use this expression 14 to simulate the field on an electrode. The signal obtained by analytical resolution fits the signal calculated with the simulation. The analytical expression is thus verified.

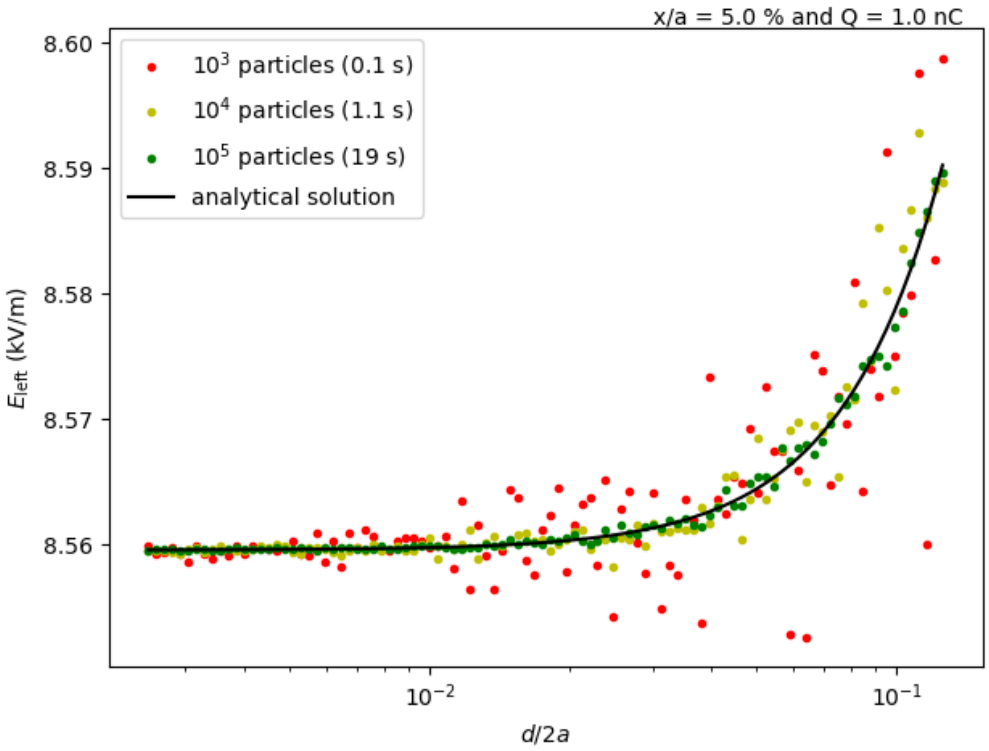

Figure 6: Evolution of the field on the left electrode with respect to $d/2a$, the field is calculated for $N_{\text{part}} = 10^3$, 10^4, 10^5, with $x/a = 5.0$ % and $\tilde{Q} = 1$ nC. The analytical solution is calculated with the expression 14, with the same parameters x and $\tilde{Q}$. The time values in the legend correspond to the time of simulation. The analytical solution fits perfectly the simulations. The more $d/2a$ is, the more particles is required to converge, which was expected.

2 Determining the properties of a beam using a BPM

2.1 Analytical determination of the position of the beam

The aim of the BPM is to give the position of the system from the signal on the four electrodes. It is known that the difference of the signal on two facing electrodes is proportional to the position in the direction of the electrodes [3]. One can show this relation with the equation 15 :

$$E_{\text{right}} - E_{\text{left}} \simeq \frac{\tilde{Q}}{2\pi L\epsilon_0}\left(\frac{1+\eta_{\text{right}}^2/4}{\rho_{\text{right}}} - \frac{1+\eta_{\text{left}}^2/4}{\rho_{\text{left}}}\right), \tag{37}$$

with $\rho_{\text{right}} = a - x$,$\rho_{\text{left}} = a + x$, and $\eta_{\text{right/left}} = \frac{d}{2\rho_{\text{right/left}}}$. Considering $\eta^2 \ll 1$, therefore :

$$E_{\text{right}} - E_{\text{left}} \simeq \frac{\tilde{Q}}{2\pi L\epsilon_0}\left(\frac{1}{\rho_{\text{right}}} - \frac{1}{\rho_{\text{left}}}\right), \tag{38}$$

$$E_{\text{right}} - E_{\text{left}} \simeq \frac{\tilde{Q}}{2\pi L\epsilon_0}\frac{2x}{a^2 - x^2}. \tag{39}$$

Finally, with $x^2 \ll a^2$:

$$E_{\text{right}} - E_{\text{left}} \simeq \frac{\tilde{Q}}{2\pi L\epsilon_0}\frac{2x}{a^2} \simeq \frac{\tilde{Q}}{\pi L\epsilon_0 a^2}x \propto x. \tag{40}$$

By using the same calculation and supposition on the sum of the signal:

$$\frac{E_{\text{right}} - E_{\text{left}}}{E_{\text{right}} + E_{\text{left}}} \simeq \frac{x}{a}. \tag{41}$$

The same expression for the two vertical electrodes gives y/a.

The equation 41 shows the same proportionality relation as the one used to determine the position in actual BPMs [3], which validates the previous hypotheses ($\eta^2 \ll 1$ and $x^2 \ll a^2$). One can verify numerically that this relation 41 gives a good approximation of x/a. For different x, the fields on the left and right electrode was calculated to obtain $\frac{\Delta E}{\Sigma E}$ with respect to x/a. The results are in the figure 7, the error is around 10^{-4}, increasing with x. This can be explained because of the approximations $x^2 \ll a^2$ and neglecting η^2.

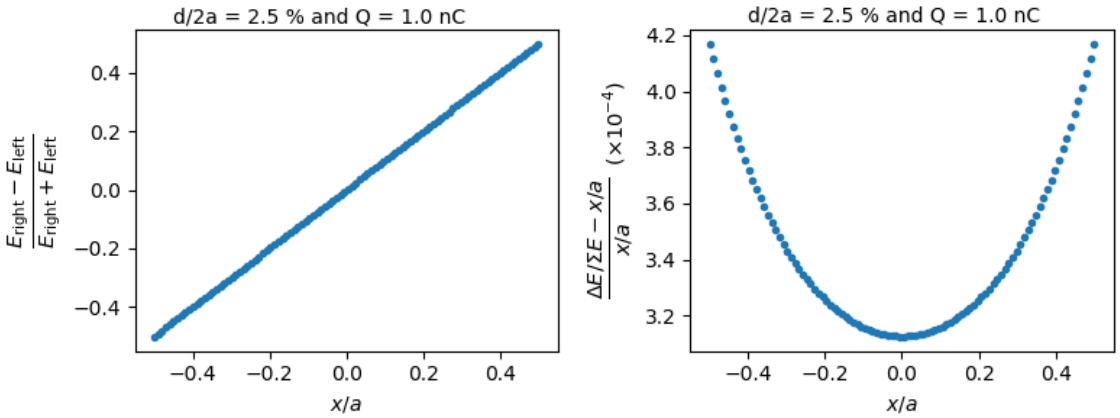

Figure 7: Evolution of the expression $\frac{E_{\text{right}} - E_{\text{left}}}{E_{\text{right}} + E_{\text{left}}}$ with respect to x/a (left) and the variation rate between $\frac{\Delta E}{\Sigma E}$ and x/a. The fields were calculated with the analytical expression 14, $d/2a = 2.5$ %, $\tilde{Q} = 1$ nC. The accuracy of the calculation of x/a with the equation 41 is around 10^{-4}.

2.2 Analytical determination of the diameter of the beam

As predicted, the BPM can give the position of the beam. The signal is also diameter dependant (equation 14 where d appears in $\eta = \frac{d}{2\rho}$). However, the diameter seems to have a low impact on the signal (cf fig. 4). The aim of this paragraph is to find an expression of d using the signal on the electrodes.

Let's first extract d from the expression 14:

$$E = \frac{\tilde{Q}}{\pi L \epsilon_0} \frac{1 - \sqrt{1-\eta^2}}{\rho \eta^2}, \tag{42}$$

$$\eta = \sqrt{2} \frac{\sqrt{\rho \frac{E}{\tilde{Q}/\pi L \epsilon_0} - \frac{1}{2}}}{\rho \frac{E}{\tilde{Q}/\pi L \epsilon_0}}, \tag{43}$$

$$d_{\text{cal}} = 2\sqrt{2} \frac{\sqrt{\rho \frac{E}{\tilde{Q}/\pi L \epsilon_0} - \frac{1}{2}}}{\frac{E}{\tilde{Q}/\pi L \epsilon_0}}. \tag{44}$$

This expression depends on x, $\tilde{Q}$, L, a and one signal E. L and a are the dimension of the BPM given by the constructor, x can be approximated by the previous relation 41, E is given by the electrode and $\tilde{Q}$ is the charge in the BPM, which can be measured via a charge detector called ICT (Integrating Charge Transformer). This expression is validated by calculating the fields expected for different value of x and d, and then apply this formula 44. There is no need of making variate y since E_{left} and E_{right} does not depend on y. The results are presented in figure 8. The figure 9 shows the precision of the method. Since x is determined approximately, this solution is not perfect. All the other parameters were input as their exact value, and the electrode's signal chosen is the left one.

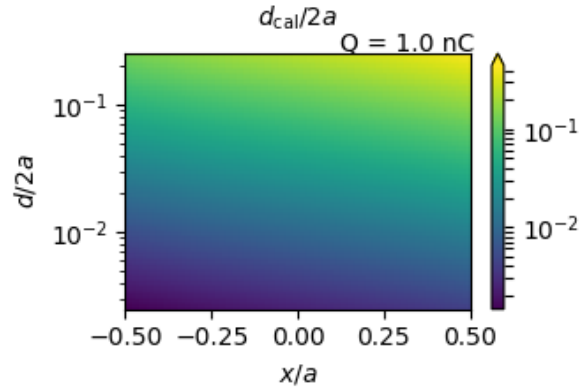

Figure 8: Map representing the results of $d_{\text{cal}}/2a$ for different set of x/a, $d/2a$. E was calculated with the analytic expression 14 with $\tilde{Q} = 1$ nC, ρ has been determined by the approximate relation 41. The values obtained seems to be close to the input $d/2a$ value.

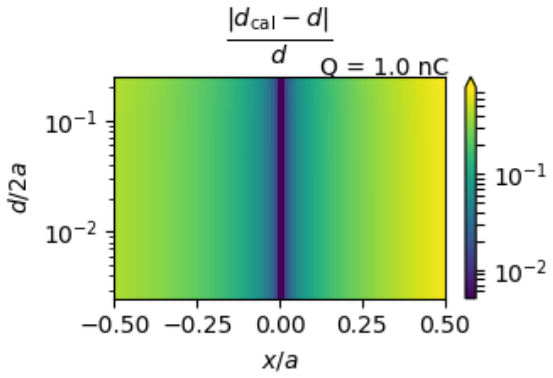

Figure 9: Map representing the variation rate between d_{cal} and the initial d. E was calculated with the analytic expression 14 with $\tilde{Q} = 1$ nC, ρ has been determined by the approximate relation 41. The accuracy of d_{cal} is below 30% and is very low in the middle of the BPM.

The figure 8 and 9 show that the expression of d_{cal} in equation 44 seems to be right, and also that the value of x determined by the relation 41 is enough to do the calculation.

The precision is not symmetrical with x. That is understandable because the expression of d_{cal} depends on the field of only one electrode, which breaks the symmetry of the relation. Therefore d_{cal} is more precise for $x < 0$, so for a beam closer to the electrode. Furthermore, the precision is minimal in the center of the BPM, which corresponds to the minimal of the error of x.

Finally, the precision does not depend on the value of d, which is an interesting behavior. However, the parameters in input $\tilde{Q}$, L, a and E are not known precisely : the previous relation 44 giving d_{cal} must not require too much precision on these parameters.

First, we will look at the charge error impact. Let's consider four beams with the following characters : $(x/a, y/a) = (5.0\ \%, 0\ \%)$, $d/2a = 0.5,\ 1.0,\ 5.0,\ 10\ \%$, and $\tilde{Q} = 1.0$ nC. The calculation of d_{cal} was made with all the exact parameters L and a, and with x calculated with the relation 41, and finally with $Q = \tilde{Q}(1-\epsilon)$. The figure 10 shows d_{cal} with the error ϵ.

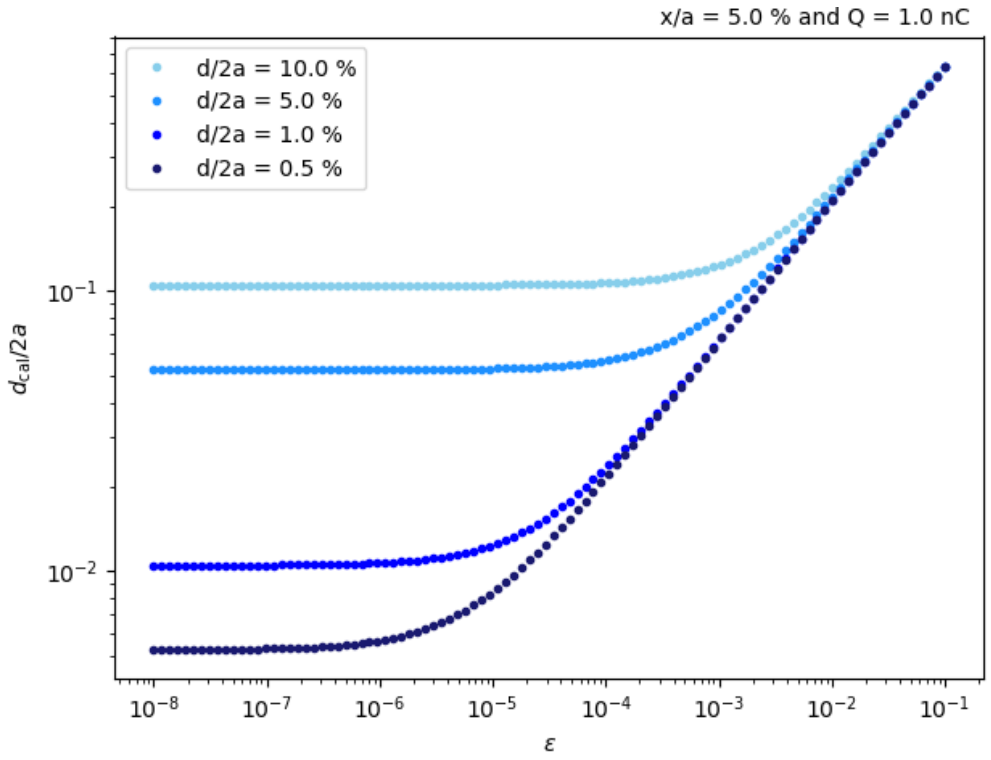

Figure 10: Evolution of $d_{\text{cal}}/2a$ with the error ϵ on the charge. The fields were calculated with the analytical expression 14, $x/a = 5.0\ \%$, $d/2a = 0.5\ \%$, $1.0\ \%$, $5.0\ \%$, $10\ \%$ and $\tilde{Q} = 1$ nC. d_{cal} was calculated with all the exact parameters except $Q = \tilde{Q}(1-\epsilon)$. For a little perturbation, $d_{\text{cal}}/2a$ converges towards the real $d/2a$. d_{cal} is incorrect for ϵ beyond a threshold that depends on the value of d. For $d/2a \sim 10.0\ \%$, the threshold is around $\epsilon \sim 10^{-4}$, so a precision of $0.01\ \%$ is required to obtain a good value. We recall that the threshold corresponds to the ϵ value where $d_{\text{cal}}/2a$ is not equal to $d/2a$, and not the ϵ corresponding to $d_{\text{cal}}/2a$ joining the other curves.

The figure 10 shows that the precision needed on the value of Q depends on the value of $d/2a$. Indeed, since d creates a tiny variation of the field, the more little d is, the more accurate the input parameters must be. In the accelerator, expects diameters around 1 mm are expected for $a = 20$ mm ($d/2a = 2.5\ \%$). For this diameter, the precision needs to be below $0.001\,\%$, which is impossible with an ICT that provides the charge with $10\,\%$ error. The expression of d_{cal} seems to be really dependant on the parameters.

To improve the determination of d, the elimination of the parameter x would be suitable, because it is calculated with an approached relation 41. To do so, let's consider the following equations :

$$\begin{cases} E_{\text{left}} \times (d/2)^2 &= \mathcal{F} \times \left((a+x) - \sqrt{(a+x)^2 - (d/2)^2} \right) \\ E_{\text{right}} \times (d/2)^2 &= \mathcal{F} \times \left((a-x) - \sqrt{(a-x)^2 - (d/2)^2} \right) \end{cases}, \tag{45}$$

$$\text{where} \quad \mathcal{F} = \frac{\tilde{Q}}{\pi L \epsilon_0}.$$

The aim is to solve this system 45 and obtain an expression of x and d depending on all the other parameters a, E_{left}, E_{right} and $\mathcal{F}$. The following calculation has been made with the library sympy on Python3. The resolution gives the following expression :

$$d_{\text{param}}(E_{\text{left}}, E_{\text{right}}, a, \mathcal{F}) = \sqrt{\frac{-\frac{E_{\text{right}}\mathcal{F}\left(2aE_{\text{right}}E_{\text{left}}(E_{\text{left}}-E_{\text{right}})+\mathcal{F}(E_{\text{right}}^2-E_{\text{left}}^2)\right)}{E_{\text{right}}E_{\text{left}}\left(E_{\text{left}}+E_{\text{right}}\right)} + 2.aE_{\text{right}}\mathcal{F} - \mathcal{F}^2}{E_{\text{right}}^2}}. \quad (46)$$

The expression 46 of d_{param} can be verified by calculating E_{left} and E_{right} for a set of x/a and $d/2a$, and with $\tilde{Q} = 1$ nC and $a = 20$ mm. The figure 11 shows the rate of change between d and d_{param} with the exact value of E_{left}, E_{right}, a, and $\mathcal{F}$. The precision of d_{param} is high with an error below 10^{-4}. However, the expression of d_{param} is less accurate for small d. That can be explained by the fact that d creates a tiny difference in the value of the electric field E_{left} and E_{right}, so the less high d is, the more computational calculus will be wrong.

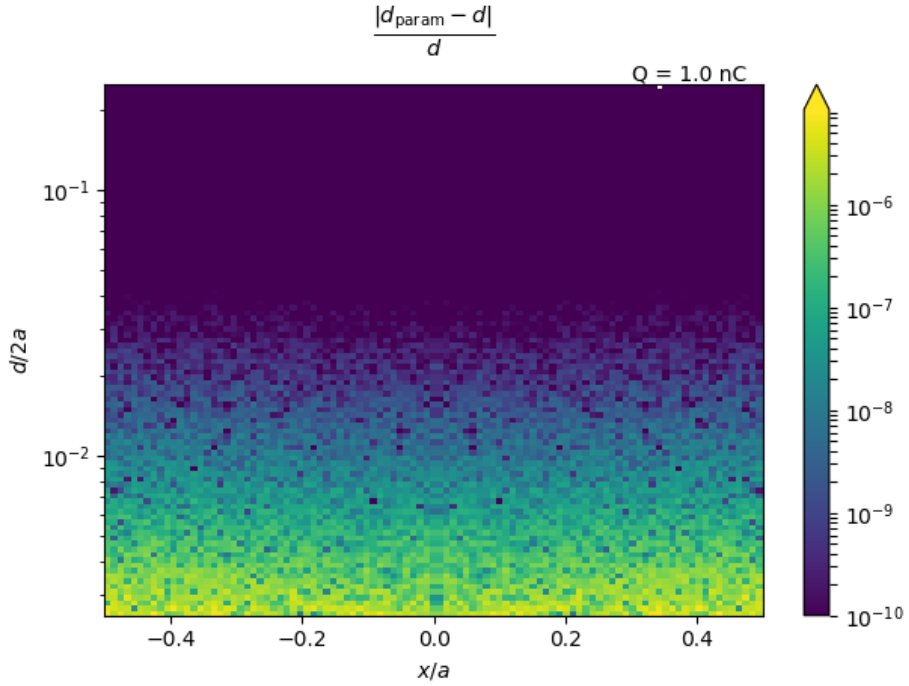

Figure 11: Accuracy of the expression of d_{param} depending on $d/2a$ and x/a. the fields have been calculated with the analytical expression 14 with $\tilde{Q} = 1$ nC. All the parameters of d_{param} were exact as input in the calculation. The error is below 10^{-4}, which indicates that the expression is right. The error is higher for little diameters d, where computational calculation founds its limit.

Let's verify the sensitivity of the expression of d_{param} 46 with respect to Q. The figure 12 shows with the same method that in the figure 10 what is the impact of an error on Q on the diameter calculation using the expression of d_{param}. No visible improvement seems to happen with this method, since the behavior of d_{param} is the same as d_{cal} one's, the precision of Q needed is about 0.001 % for $d/2a = 2.5$ %. Hence, the sensitivity of the expression of d_{cal} is not the consequence of an error on x, but a sensitivity with respect to the charge $\tilde{Q}$. The same study can be made to determine the sensitivity with respect to the other parameters E_{left}, E_{right}, L and a. The evolution of d_{param} is the same that the one shown in figure 12, so the expression of d_{param} is highly sensitive for all the parameters.

The expression of d_{param} is really dependant on the parameters because the diameter of the beam creates a tiny contribution to the field. In order to improve the results of d_{param}, the effect of d on the field must be increased. The developed expression of $E_{\text{electrode}}$ 15 shows that d contributes to the field with $\eta = \frac{d}{2\rho}$. Hence, The accuracy of d_{param} will increase with η. To demonstrate this behavior, a diameter $d = 1$ mm is chosen and the fields are calculated for some sizes a. Then, an error on Q is introduced in the calculation of d_{param}. The result is shown in figure 13. The same figure was made for different value of x and no dependency has been demonstrated.

The behavior of the curves is similar to the one of the curves in figure 12, which was expected since the field contribution that is diameter dependant is $\eta \sim d/2a$. However, this figure gives the value of

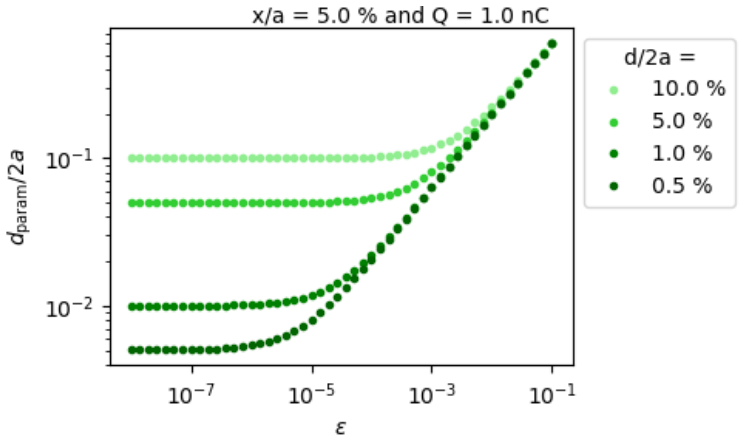

Figure 12: Evolution of $d_{\text{param}}/2a$ with an error ϵ on the charge. The fields have been calculated with the analytical expression 14, $x/a = 5.0$ %, $d/2a = 0.5$, 1.0, 5.0, 10.0 % and $\tilde{Q} = 1$ nC. d_{param} has been calculated with all the exact parameters except $Q = \tilde{Q}(1-\epsilon)$. This figure is to compare to the figure 10, the two figures present the same behavior and the same thresholds. The sensitivity of d_{cal} is not solved by the expression d_{param}.

$d/2a$ that corresponds to the error expected. The parameters that gives the most accurate d_{param} is $d/2a = 1$, which means a BPM with the same radius than the beam. With a precision of 0.1 % on the charge, $d/2a > 20$ % can be determined. Hence, huge diameter will be measurable.

However, the calculation of the field $E_{\text{electrode}}$ 14 is valid for tiny d since the hypothesis of the overlap between the electrode and a cylinder is valid for $v/a \times 0.4 \ll 1$. With $d/2a \sim 1/16$, $v/a \times 0.4 = 0.1$ so the hypothesis can be considered as valid for $d/2a < 1/16$. Thus, the expression of d_{param} will not give the diameter with precision for a $d/2a$ too large. However, the expression of $E_{\text{electrode}}$ gives the trend of E with d, even though it does not give the exact value of the field. So, even though the figure 13 is not right for large $d/2a$, it is relevant to estimate what precision is needed to determine the diameter. In order to obtain this value, the field should be calculated without approximations.

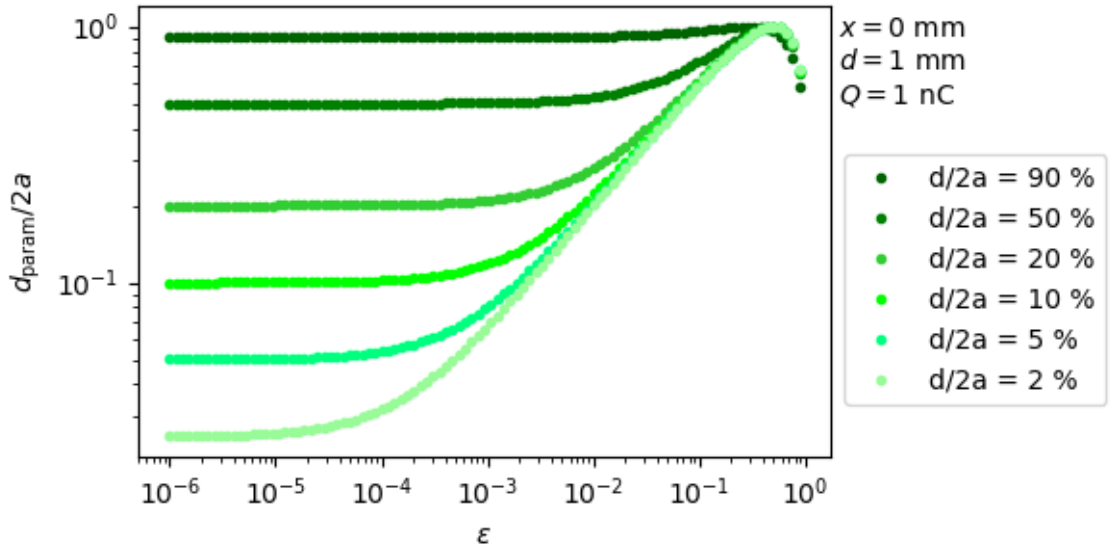

Figure 13: Evolution of $d_{\text{param}}/2a$ with an error on the charge. The fields have been calculated with the analytical expression 14, $x = 0$ mm, $d = 1.0$ mm, and $\tilde{Q} = 1$ nC. The only varying parameter is the radius of the BPM a. d_{param} has been calculated with all the exact parameters except $Q = \tilde{Q}(1-\epsilon)$. The higher d is, compared to a, the less accurate the parameters can be. The greatest accuracy achievable is for $d = 2a$, which means the BPM has the same radius than the beam.

The study of the sensitivity of d_{param} showed that d_{param} is highly sensible to the parameters. This sensibility decreases when $d/2a$ increases. Hence, the more the noise can be reduced on the parameters, the more tiny beams will be accessible.

All this study was made with an error on only one parameter : the charge. However, an error on

every parameter should create the same figure for d_{param}. To verify that assumption, let ϵ be the global error, and each parameter is given with an error ϵ_i so that $\epsilon^2 = \sum_i \epsilon_i^2$. The ϵ_i were calculated with four random angles that give the position of a point of a sphere in five dimensions. The coordinates of the point multiplied by $\pm\epsilon$ will give the ϵ_i. d_{param} is then calculated with the error on each parameters. In figure 14, d_{param} has been plotted with respect to ϵ.

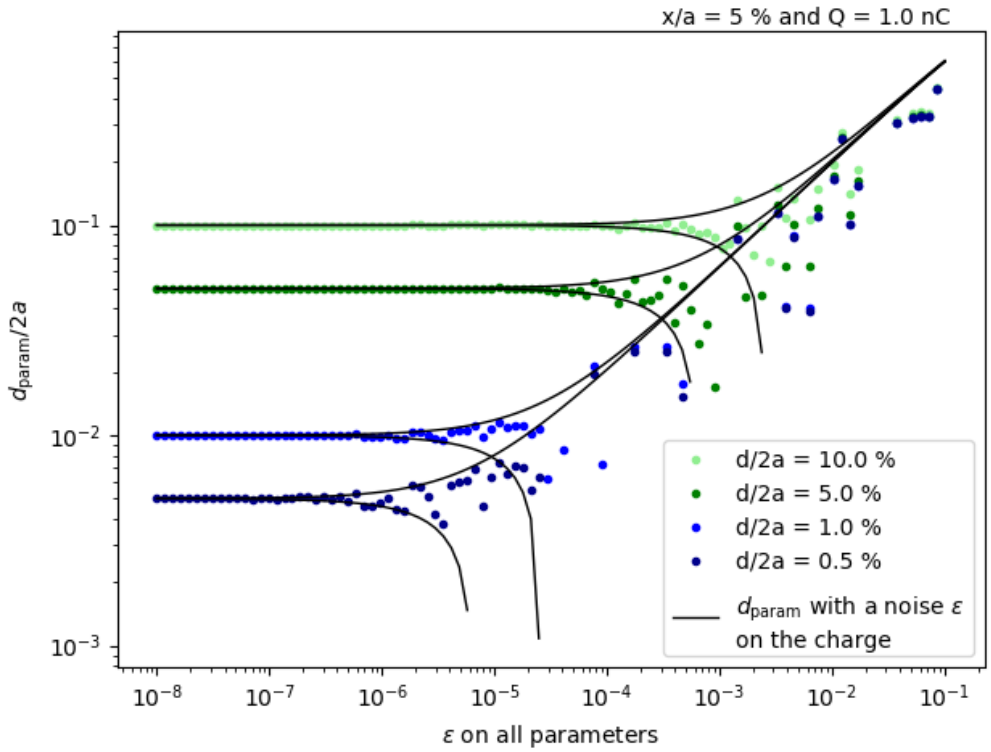

Figure 14: Evolution of d_{param} with an error on every parameters $\tilde{Q}$, E_{left}, E_{right}, a and L. The black lines corresponds to the value of d_{param} with an error of $\pm\epsilon$ on the charge. The increasing lines corresponds to $Q = \tilde{Q}(1-\epsilon)$ and the decreasing lines corresponds to $Q = \tilde{Q}(1+\epsilon)$. The points are mostly between the black lines, which means that the study of the sensitivity can be limited to the study of the sensitivity of one parameter, here the charge.

This figure 14 shows in black the two limits of d_{param} calculated with $Q(1\pm\epsilon)$. For one d, the d_{param} calculated are mostly in this zone, which shows that the previous study that analyses the sensibility of d_{param} on one parameter is relevant.

3 Reduction of the noise using the ring of the accelerator

3.1 Presentation of the ring

In the previous section, the influence of the noise on the expression of d_{param} was exposed. Since the resolution of the BPMs or the ICT (charge measuring device) is given by the constructor, the only way to decrease the impact of the noise is to repeat the measurements and perform a statistic treatment on the data. There are two ways to proceed : the first one is to do the measurement on the same beam, the second one is to do the measurement on several beams. This study focuses on the first point. We recall that previous works on determining diameter information with a BPM use also several measurements [1], [2].

In the ThomX accelerator, the beam can propagate in an accelerator section (LINAC), a transfer line, a ring and an extraction line (cf fig 15). At least one BPM is installed in each part. To measure the same beam, the ring seems to be the greatest place since the same beam will loop around 4.10^5 times. The BPMs in the ring are able to measure the beam every two loops, so it can produce 2.10^5 measurements : the noise can be heavily reduced. All the BPMs in the ring have the same radius a and length L.

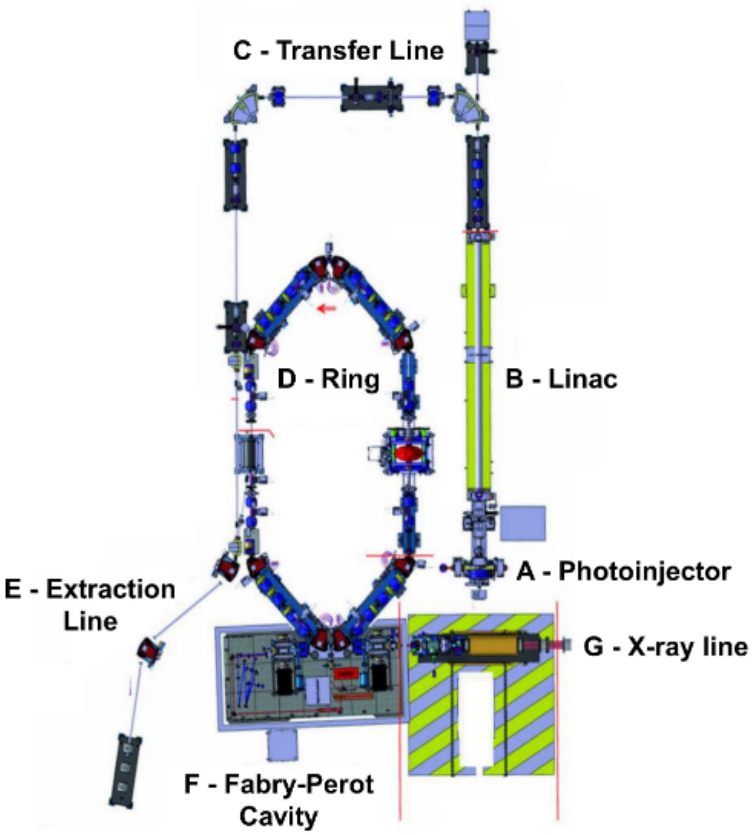

Figure 15: Diagram representing the ThomX facility, from [4].

To understand what statistical treatment is valuable, the study of the properties of a beam in a rings is relevant. The beam will have the same diameter for every loop at a giving point in the ring. Moreover, the beam is highly centered in the tube, since a tiny fluctuation of the position would be repeated a huge number of times, and the beam would leave the ring. Let's first consider that the beam is centered in the ring ($x = y = 0$ mm). Finally, the beam looses a tiny amount of charge during the propagation, this amount is supposed to be negligible.

With all these suppositions, the signal on all the electrodes of a BPM is a constant during the loops. However, at each loop, a noise is applied on the signal. To simulate this noise, the theoretical signal can be multiplied by $(1 + \delta E)$ with δE following a normal law with a zero mean and a standard

deviation σ. The field applied on an electrode of the BPM number i of the ring and during the loop number j is written :

$$E^{\mathrm{i}}_{\mathrm{l,r,b,t}}[\mathrm{j}] = E_{\mathrm{electrode}}(x=0, d_{\mathrm{i}}, Q, L, a) + \delta E^{\mathrm{i}}_{\mathrm{l,r,b,t}}[\mathrm{j}], \tag{47}$$

with l,r,t,b referring to the left, right, bottom and top electrode.

Rather than looking at the signal on one electrode, the sum of the signal on two opposed electrodes is more suitable : with a zero noise, this sum is symmetric with x, which will be interesting in the following. The mean of this sum is giving an approached value of the sum of the signal with zero noise.

$$\langle E^{\mathrm{i}}_{\mathrm{l,b}}[\mathrm{j}] + E^{\mathrm{i}}_{\mathrm{r,t}}[\mathrm{j}]\rangle_{\mathrm{j}} = \langle 2E_{\mathrm{electrode}}(x=0, d_{\mathrm{i}}, Q, L, a)\rangle_{\mathrm{j}} + \langle \delta E^{\mathrm{i}}_{\mathrm{l,b}}[\mathrm{j}] + \delta E^{\mathrm{i}}_{\mathrm{r,t}}[\mathrm{j}]\rangle_{\mathrm{j}}, \tag{48}$$

$$= 2E_{\mathrm{electrode}}(x=0, d_{\mathrm{i}}, Q, L, a), \tag{49}$$

$$= \frac{\tilde{Q}}{L\pi\epsilon_0}\frac{a-\sqrt{a^2-(d_{\mathrm{i}}/2)^2}}{(d_{\mathrm{i}}/2)^2}. \tag{50}$$

Since a and L are constant for a given BPM, the charge is the only parameter to calculate the diameter. However, there is no ICT in the ring of ThomX, so no ways to obtain $\tilde{Q}$ with enough precision as demonstrated in the previous section. To avoid the charge parameter, this mean can be divided by the mean of the two opposed signal of the first BPM in the ring. Since the charge is constant during the propagation in the ring, the charge will disappear.

$$\frac{\langle E^{\mathrm{i}}_{\mathrm{l,b}}[\mathrm{j}] + E^{\mathrm{i}}_{\mathrm{r,t}}[\mathrm{j}]\rangle_{\mathrm{j}}}{\langle E^{1}_{\mathrm{l,b}}[\mathrm{j}] + E^{1}_{\mathrm{r,t}}[\mathrm{j}]\rangle_{\mathrm{j}}} = \frac{(d_1/2)^2}{(d_{\mathrm{i}}/2)^2}\frac{a-\sqrt{a^2-(d_{\mathrm{i}}/2)^2}}{a-\sqrt{a^2-(d_1/2)^2}}, \tag{51}$$

$$\simeq \frac{1+\eta_{\mathrm{i}}^2/4}{1+\eta_1^2/4}, \tag{52}$$

$$\eta_{\mathrm{i}}^2 - \eta_1^2 \simeq 4\left(\frac{\langle \Sigma E^{\mathrm{i}}\rangle}{\langle \Sigma E^{1}\rangle} - 1\right). \tag{53}$$

The limited development have been made considering $\eta^2 \ll 1$, where in the ring of ThomX, $\eta < 10$ %. The data $\frac{\langle \Sigma E^{\mathrm{i}}\rangle}{\langle \Sigma E^{1}\rangle}$ seems to give an information on the evolution of the diameter in the ring, since $\eta_{\mathrm{i}}^2 - \eta_1^2 = \frac{d_{\mathrm{i}}^2 - d_1^2}{(2a)^2}$. This method cannot give the value of d_{i} since the value of d_1 is not known.

Even though the value of the diameter cannot be determined in every BPM, an image of the variation of these diameter can be produced. This information is really interesting because it gives an information on the shape of the beam, which gives also an information on the magnet force used in the ring, which is called the lattice of the ring. The other methods to measure the lattice of a ring is first a local measurement : one places a magnetometer on every magnet and test the magnet. This method is long since every magnet must be tested one by one. Another method to determine the lattice of the ring is to change magnet strength and verify whether the beam reacts normally or not. This process often looses the beam. The method that is discussed in this study would give the shape of the lattice very quickly (10^5 loops in ThomX are done in 5 ms) and without loose the beam.

This method supposes the following hypotheses :

- The number of loop N_{loop} is sufficient for $\frac{\langle \Sigma E^{\mathrm{i}}\rangle}{\langle \Sigma E^{1}\rangle}$ to approach the mathematical expectation with enough precision;
- The beam is centered in the tube;
- The charge of the beam is constant during the propagation in the ring.

The following paragraphs will estimate the validity of these hypotheses.

3.2 Convergence with the number of loops

The first hypothesis to verify is the convergence of $\frac{\langle \Sigma E^{\mathrm{i}} \rangle}{\langle \Sigma E^{1} \rangle}$ towards its mathematical expectation, that is $2E_{\mathrm{electrode}}(x = 0, d_{\mathrm{i}}, Q, L, a)$. Since $d/2a$ has a very tiny impact on $E_{\mathrm{electrode}}$, we expects that two close diameters will have close mathematical expectations. To make a difference between two close diameters, enough loops will give a sufficient approximation the mathematical expectation with the mean $\frac{\langle \Sigma E^{\mathrm{i}} \rangle}{\langle \Sigma E^{1} \rangle}$.

To determine the number of loops that is needed, a beam in a ring is simulated. Since the beam is centered, the only variables are the radius of the BPM $a = 5.4$ mm and the diameters of the beam in each BPM. In ThomX, there are 12 BPMs in the ring. The diameters of the beam are given by another simulation program called MadX that gives the parameters of the beam at every step of its propagation.

MadX simulates the beam with an ellipse with σ_x the semi axis on the x direction and σ_y the semi axis on the y direction. MadX returns at each point of the ring the value of the β function and the emittance ϵ, that are traditionnal parameters used to describe a beam in an accelerator [5]. These parameters are related to the semi axis by $\sigma_x = \sqrt{\beta_x \epsilon}$. Since ϵ is a constant in the ring, $\sigma_x \propto \sqrt{\beta_x}$, which evolves during the propagation. Hence, with supposing $d = 2\frac{\sigma_x + \sigma_y}{2}$, the diameter values can determined in the ring.

The field $E_{\mathrm{electrode}}(x = 0, d_{\mathrm{i}}, Q, L, a)$ can be calculated N_{loop} times in every BPM. For every loop, a noise δE following a normal law is added (with a zero mean, a standard deviation $\sigma = 0.1$ and an amplitude $\mathcal{A}$). In figure 16 is shown $\frac{\langle \Sigma E^{\mathrm{i}} \rangle}{\langle \Sigma E^{1} \rangle}$ and the mathematical expectation for two different amplitudes $\mathcal{A} = 10\,\%$; $100\,\%$. An amplitude $\mathcal{A} = 10$ % corresponds to a noise around 1 %, since $\sigma = 0.1$.

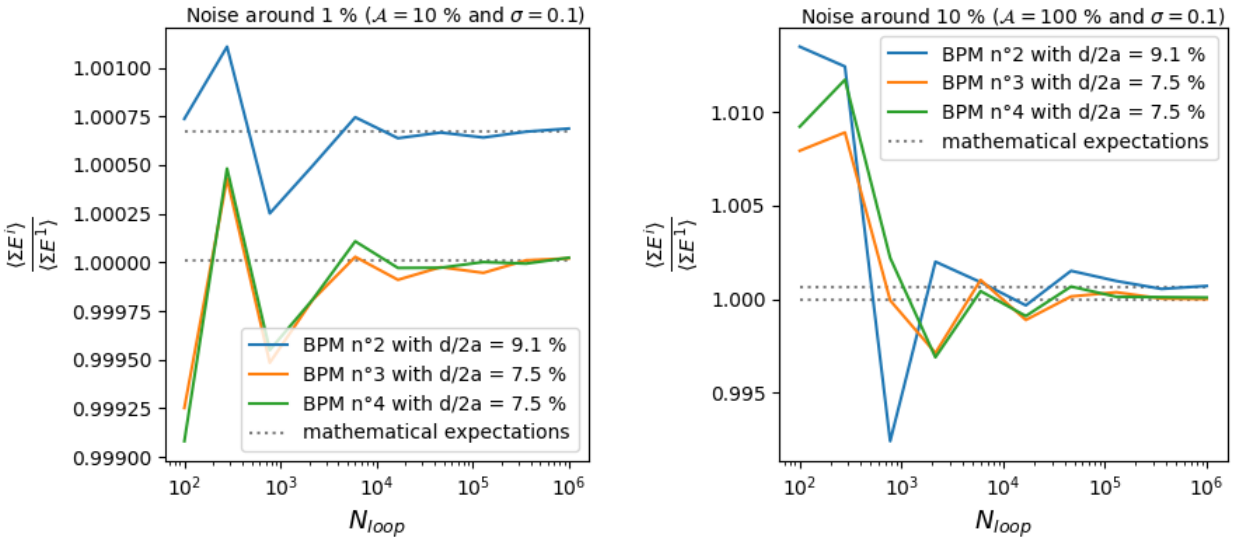

Figure 16: Evolution of the ratio $\frac{\langle \Sigma E^{\mathrm{i}} \rangle}{\langle \Sigma E^{1} \rangle}$ with the number of loops for a centered beam. On the left, the simulation was performed with a noise on the fields around 1 % ($\sigma = 0.1$ and $\mathcal{A} = 10$ %), on the right, the simulation was performed with a noise on the fields around 10 % ($\sigma = 0.1$ and $\mathcal{A} = 100$ %). In both cases, the ratio is converging towards the mathematical expectation $\frac{E(d_{\mathrm{i}})}{E(d_1)}$, however the number of loop needed to do the difference depends on the noise : with a noise around 1 %, the two $d/2a = 9.1$ % and 7.5 % are distinguishable with $N_{\mathrm{loop}} = 10^4$, when for a noise around 10 % the separation happens around $N_{\mathrm{loop}} = 10^5$. The order of magnitude of the expectation variations is around 10^{-4}, that is why N_{loop} must be high enough to approach the expectation with an accuracy around 0.01 %.

The bigger N_{loop} is, the closer the mean from the expectation will be, which was an expected behavior. Moreover, the amplitude of the noise plays a role in the convergence of the mean : the less

the noise is, the quicker the mean will converge. The nature of the noise in ThomX is not known with precision, the study will focuses on a 1 % noise ($\mathcal{A} = 10$ %) that seems to be the order of magnitude of this noise. To have a more global vision, one can do the same simulation with respect to the position in the ring. These results are shown in figure 17.

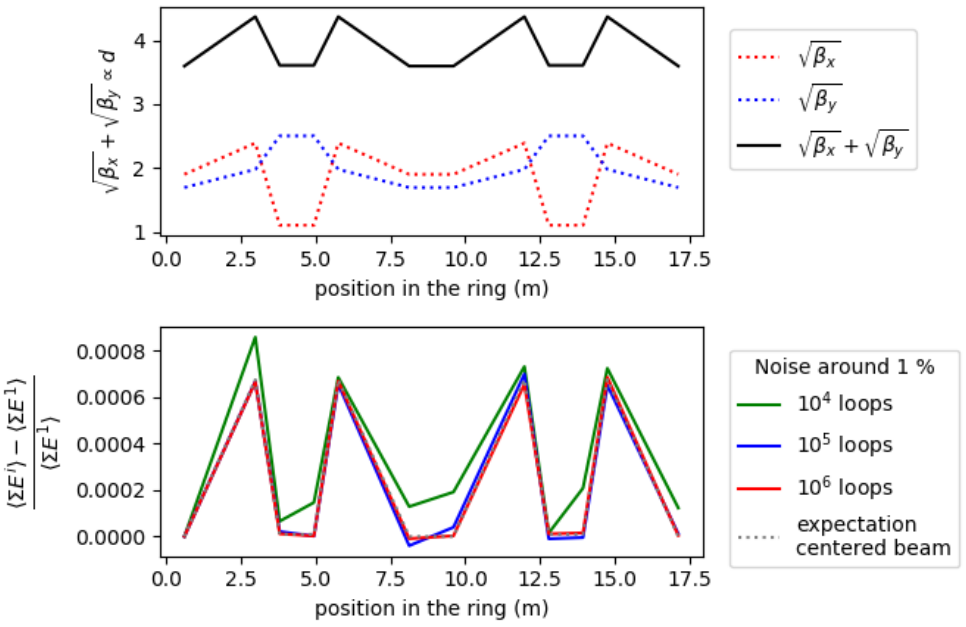

Figure 17: Evolution of the ring lattice (above graph) and evolution of the ratio $\frac{\langle \Sigma E^i \rangle}{\langle \Sigma E^1 \rangle}$ along the ring for different N_{loop} and a centered beam. The noise introduce is around 1 % with $\sigma = 0.1$ and $\mathcal{A} = 10$ %. As expected, the ratio is converging towards the mathematical expectation with N_{loop}. The evolution of the ratio is similar to the ring lattice $\sqrt{\beta_x} + \sqrt{\beta_y}$ and thus give the shape of the lattice.

The figure 17 shows the difference between $\frac{\langle \Sigma E^i \rangle}{\langle \Sigma E^1 \rangle}$ and 1 (the ratio for the first BPM). The shape of the ratio of the mean is converging toward the mathematical expectation with the number of loop N_{loop}, which was already illustrated in the figure 16. This figure 17 shows also that the shape of the lattice $(\sqrt{\beta_x} + \sqrt{\beta_y})$ can be obtained with this method.

Therefore, the convergence of the ratio of the mean fields depends on the number of loops and on the amplitude of the noise. However, this method depends also on the ratio $d/2a$. The lower $d/2a$ is, the less impacted the fields will be and the more loops will be needed. To verify that supposition, the resolution of this method will be calculated.

Let's consider that with a difference of fields ΔE, two diameters will be distinguishable if their difference is above $\Delta d = \Delta E / \partial_d E$. Hence, with the difference $\Delta E = \langle \Sigma E^i \rangle - 2E_{\text{electrode}}(x = 0, d)$, the resolution on d will be :

$$\frac{\Delta d}{d} = \frac{\langle \Sigma E^i \rangle - 2E_{\text{electrode}}(x = 0, d)}{2d\ \partial_d E(x = 0, d)}, \tag{54}$$

where $\frac{\Delta d}{d}$ represents the relative gap of diameters that is distinguishable with this method. To obtain this resolution, $\langle \Sigma E^i \rangle$ is calculated for some $d/2a$ and some N_{loop}. These values will give a gap between the mean and the expectation, but this gap depends on the simulation. By repeating this simulation, the mean gap between the expectation and the mean fields appears and give the expected resolution. The figure 18 shows the results for 25 repeated simulations. The figure 19 shows some particular lines in the figures 18 and their possible extensions.

In the figure 18, the resolution increase with N_{loop} and $d/2a$ as expected. However, the point with the same resolution are situated on a line in a logarithmic scale. To have a better vision of the resolution, a linear regression is done on the points of the map that are close to a resolution, such as

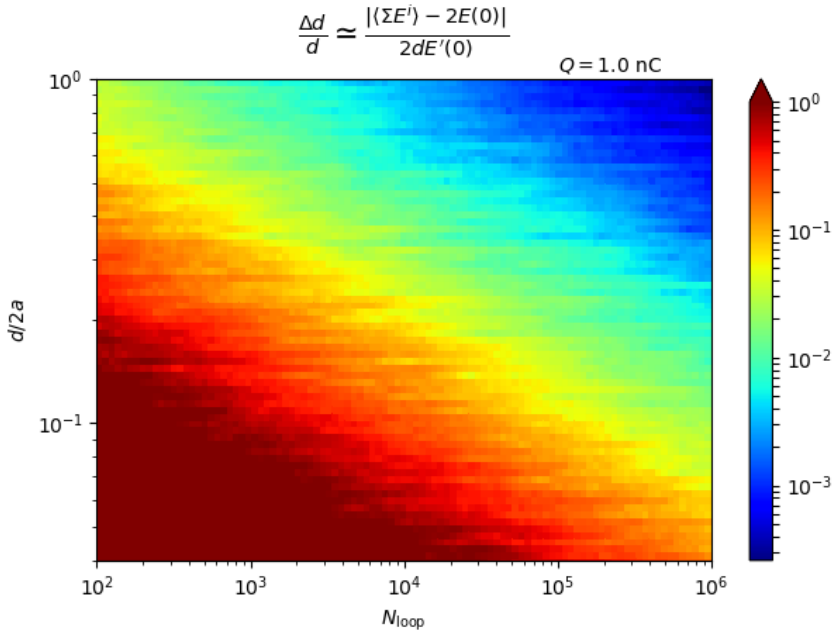

Figure 18: Evolution of the resolution $\frac{\Delta d}{d}$ with N_{loop} and $d/2a$ for a centered beam. The noise introduced is around 1 % ($\sigma = 0.1$ and $\mathcal{A} = 100$ %), and $\langle \Sigma E^{\text{i}} \rangle$ was calculated 25 times to obtain a flatten map. As expected, the resolution is increasing with N_{loop} and with $d/2a$. Points with a same resolutions are placed on a line and that all the lines have the same slope.

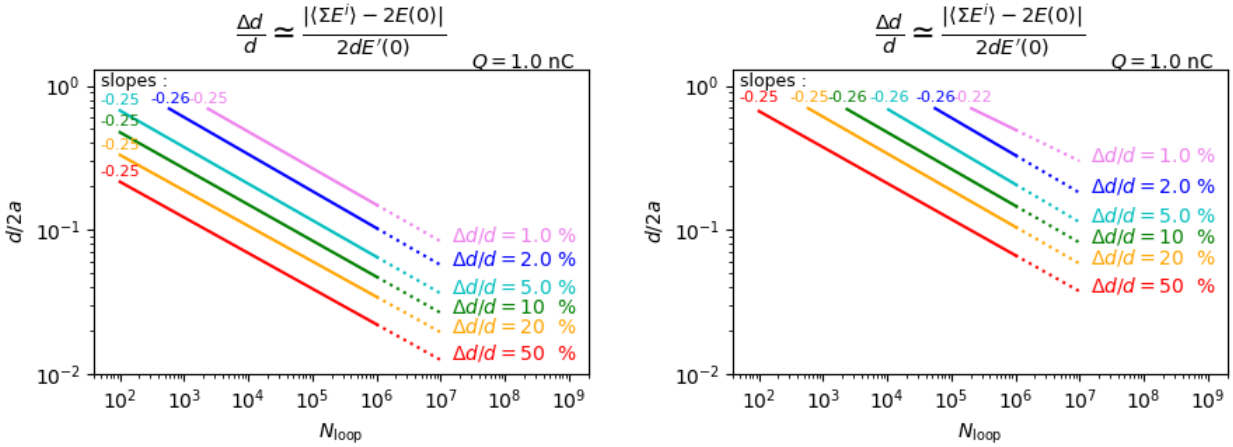

Figure 19: Evolution for a centered beam of the resolution with N_{loop} and $d/2a$, which corresponds to the linear regression of the points in the figure 18 that are at most 10 % close to the resolutions (in full lines). The lines have been extended (dashed lines) to give assumed resolutions for more than $N_{\text{loop}} = 10^6$. On the left, the simulations were performed with a noise on the fields around 1 % ($\sigma = 0.1$ and $\mathcal{A} = 10$ %), on the right, the simulations were performed with a noise on the fields around 10 % ($\sigma = 0.1$ and $\mathcal{A} = 100$ %). The slopes of the lines are similar around 0.25, which means that for a given resolution, with one order of magnitude more in number of loop , one can determine a quarter of order of magnitude in $d/2a$ less. One can also see the effect of the noise on the resolution : with 10 times less noise, one can determine $d/2a$ with an half decades less for the same resolution.

10 %. That calculus will lead to the results in figure 19. In full lines, the regression where the points were and in dotted lines the assumption by extending the full lines.

In the figure 19, some behavior are noticeable : in order to increase the resolution with a 10 factor, two order of magnitude more in number of loop are needed. This result corresponds to the law saying that the convergence of a normal distribution of probability is proportional to $\sqrt{N_{\text{loop}}}$. Moreover, for a given resolution, with one order of magnitude more in number of loop, the $d/2a$ achievable is a quarter of order of magnitude less. Thus, it is really difficult to have enough resolution for tiny $d/2a$. Finally, with dividing the noise amplitude by 10 for a given N_{loop}, with the same resolution, the $d/2a$ achievable are a half of order of magnitude less.

Since the resolution given with $\Delta d/d$ corresponds to the resolution for $\langle E^i \rangle$, the resolution of $\frac{\langle \Sigma E^i \rangle}{\langle \Sigma E^1 \rangle}$ will be the same because the noise is not correlated between the BPMs. In ThomX, the diameter of the beam in the ring is around $d/2a \sim 10^{-1}$. Depending on the noise introduced by the BPMs, this methods will give a resolution between 10 % and 20 % for an amplitude $\mathcal{A} = 10$ %, but it will not have enough resolution with an amplitude of $\mathcal{A} = 100$ %. Since the noise in ThomX is not understood, a deeper study of the noise in the BPM is needed to confirm the 1 % noise and thus conclude on the possibility of this method to visualise the lattice in the ring.

3.3 Fluctuation of the position of the beam

The previous section assumed that the beam was centered during its propagation in the ring. This hypothesis was supposed since a tiny gap in the position of the beam would be repeated for each loop, and so the beam would disappear. However, the position of the beam can fluctuate around the center of the BPM. These tiny fluctuations should not have a great impact on the mean of the fields, this section will simulate these fluctuations to verify their impact.

The field on each electrode is calculated with the diameter predicted by MadX simulation, and with the position spread randomly following a normal law with a mean zero and a standard deviation δ_x. A 1 % noise of amplitude with $\mathcal{A} = 10$ % is applied to every field. The results are shown in figure 20.

The figure 20 shows that for tiny δ_x, the mean fields converge towards the mathematical expectations of a centered beam. The hypothesis considering that the fluctuations are negligible is thus verify for δ_x small enough, which corresponds to $2\delta_x/d < 50$ % with $d/2a \sim 10$ %, $\mathcal{A} = 10$ % and $\sigma = 0.1$. For further δ_x, the hypothesis seems to deviate from the expectations. The new expectation can be calculated with the following formula :

$$\mathbb{E}(E_{\text{l}}^i + E_{\text{r}}^i) = \int_{x_{\text{i}}} \left(E_{\text{l}}^i + E_{\text{r}}^i\right) \times \text{p}(x_{\text{i}})\, \text{d}x_{\text{i}}, \tag{55}$$

where $\text{p}(x_{\text{i}})$ is the density of probability to obtain the position x_{i}.

The density $\text{p}(x_{\text{i}})$ is measurable with the BPM since they are sensible to the position of the beam. The density can be approximated with the N_{loop} measurements of the position. However, the calculation will implies some errors : the value of x_{i} for each loop will be approached, the density could not have converged enough after N_{loop} and a potential numerical integration will also introduce an error on the mathematical expectation. Since the precision needed on the expectation is around 10^{-4}, the precision of the calculation is not certain.

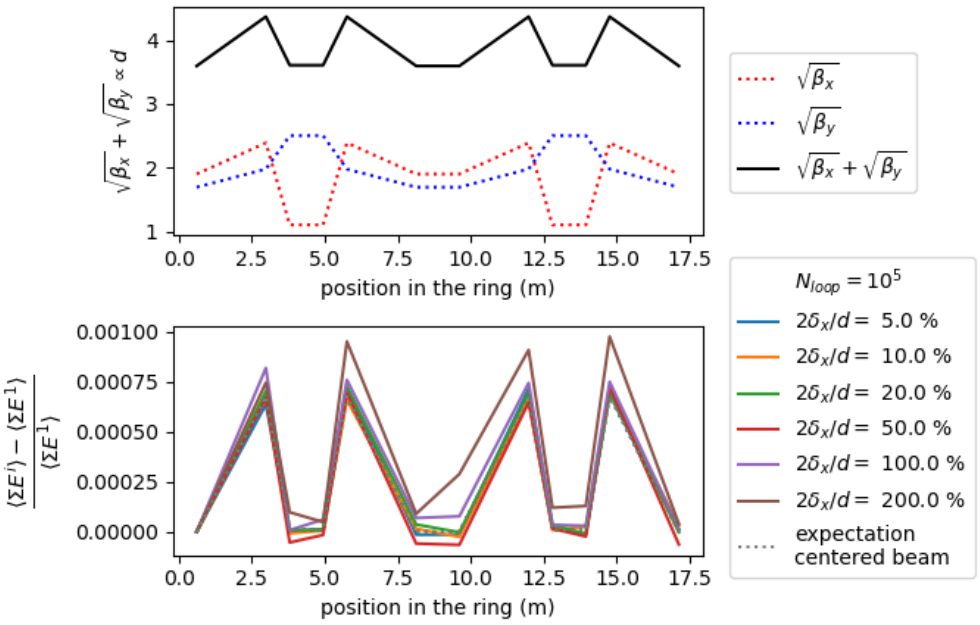

Figure 20: Evolution of the ring lattice (above graph) and evolution of the ratio $\frac{\langle \Sigma E^{\mathrm{i}} \rangle}{\langle \Sigma E^1 \rangle}$ along the ring for different N_{loop} and fluctuations in positions following a normal law with a zero mean and a standard deviation δ_x. The noise introduce is around 1 % with $\sigma = 0.1$ and $\mathcal{A} = 10$ %. The less fluctuating the position is, the more close to the expectation for a centered beam the ration is. The evolution of the ratio keeps to be similar to the ring lattice $\sqrt{\beta_x} + \sqrt{\beta_y}$ for tiny deviation $\delta_x < 50$ % and thus give the shape of the lattice.

3.4 Prefactor elimination

The aim of the ratio $\frac{\langle \Sigma E^{\mathrm{i}} \rangle}{\langle \Sigma E^1 \rangle}$ is to eliminate the prefactor $\mathcal{F} = \frac{\tilde{Q}}{\pi L \epsilon_0}$. However, this division is not necessary avoiding this prefactor, because of $\tilde{Q}$ and L.

First, the charge of the beam is not exactly constant during the propagation. Some electrons are lost, which means that the absolute charge is decreasing. Even though this charge loss is small, a tiny error on one parameter can blur the impact of d on the field. The figure 13 shows that an error above 10^{-4} on the charge with a ration $d/2a = 10$ % will blur the d impact. Hence, a small deviation of the charge can blur the determination of d.

One way to solve this problem is to calculate $\langle \frac{\Sigma E^{\mathrm{i}}}{\Sigma E^1} \rangle$ instead of $\frac{\langle \Sigma E^{\mathrm{i}} \rangle}{\langle \Sigma E^1 \rangle}$. Doing the ratio before the mean will simplify the charge loop by loop. The charge loss at each loop is N_{loop} times less important than the charge loss between the first and the last loop. Even though this calculation avoids the problem of the charge, it requires more information on the noise and on the correlation between the fluctuation of the position in each BPM.

Finally, the charge is not the only parameter that can deviate the mathematical expectations. The length of the electrodes L is not exactly the same for every electrodes. In ThomX ring, the electrodes are 2 cm long. The precision should be really high on this parameter to avoid a blur of the d impact. As well as for the charge, for $d/2a \sim 10$ %, one need a precision of 10^{-4}, so a precision of 1 μm on 2 cm, which is not possible. The error introduced is a systematic error. Hence, it can be determined and corrected. One way to proceed is to analyse the signal returned by the BPM, since the field applied on the electrode will produce a tension correlated to the impedance of the device. This impedance is determined in particular by the shape of the electrode. Further studies could give a precise method to determine the length of each electrode with precision. Another way to proceed is to divide each signal by all the signals from the other BPMs. A statistical treatment could be applied to determine the length gaps between all the electrodes of the BPMs.

4 Conclusion and perspectives

The aim of this study was to evaluate the sensibility of a BPM to the diameter of the beam. If a single measurement of the beam using a BPM seems to be irrelevant, an accumulation of measurements could give an information on the beam, even though this information is relative to a reference (the first BPM).

The accuracy of the information will depend on several factors : the size of the beam $d/2a$, the number of measurement N_{loop}, the amplitude $\mathcal{A}$ and the shape of the noise on the electrodes, the amplitude of fluctuations of the beam position δ_x, and the precision on the length of the electrodes. In the case of ThomX, the factors are not all known. Simulations with MadX give the order of magnitude expected $d/2a = 10$ %, the number of loop is already predicted to be 4.10^5 so one can achieve 2.10^5 measurements. However, since ThomX is not yet a running machine, some value are missing to determine other factors : the shape and amplitude of the noise is uncertain, even if other internal studies on other beams have shown a noise around 1 % ; the amplitude of fluctuations is not known, even if one can suppose that they should not be more than one diameter regarding the actual diameter $d/2a = 10$ %. Finally, the length of the electrodes 2 cm long is not accurate with less than 10 μm, the determination of the length of these electrodes should be done after the machine starts. Hence, with the available data, the BPM should be able to make the difference between two diameters with a gap of 10 %, considering a good calibration for the electrodes lengths.

The object of interest of the study was a particular type of beam with a circular section. The study should be extended with an elliptical beam, with d_x and d_y the semi axis of the beam. The calculations could lead to the possibility of measuring the two transverse diameters, which could give a preciser information on the lattice.

Moreover, the charge distribution of the beam was assumed to be uniform, which is not the case in an accelerator. Other studies, such as Miller's [1] or Kurennoy's [6], gives the calculation in the case of an elliptic beam and with a gauss distribution in charge. This model seems to be much accurate, but the calculations cannot reveal the diameters d_x or d_y, but only $d_x - d_y$. Considering a uniformly charged beam could thus be a way to obtain a value for d_x and d_y.

Finally, this study cannot confirm that the estimated resolutions for high $d/2a$ ratio are corrects, since the calculus is based on a beam close to the BPM. Kurrenoy's work [6] studies the particular case of high $d/2a$, that implies non linearity.

This study lacks experimental data to confirm its conclusion. A deep study of the noise in the BPM would be a good step to know the precision of the method. Moreover, experimental data of a propagation in the ring would provide the confirmation of the efficiency of the method. Further calculations can also improve the existing method : the study of other statistical treatments giving the diameter with more precision ; the development of numerical programs to calculate the mathematical expectation when calculations are not possible ; the development of an artificial intelligence taking all the fields in input and giving the diameters in output. Finally, this method could be extended to other accelerator with either high $d/2a$ or high N_{loop}, SOLEIL is an interesting machine since N_{loop} can be 10^8 or 10^9, however little the diameter might be ($d/2a \sim 1$ %).

This study has shown the sensitivity of the BPMs to the diameter of the beam, and a statistical treatment was determined to obtain the lattice of the ring. Further development, especially experimental, can confirm the efficiency of this statistical treatment.

References

[1] Roger H. Miller, J. E. Clendenin, M. B. James, and J. C. Sheppard. Nonintercepting emittance monitor. Conf. Proc. C, 830811:602–605, 1983.

[2] Ralph Assmann, Bernd Dehning, and John Matheson. Use of movable beam position monitors for beam size measurements. 01 2000.

[3] M. Wendt. Bpm systems: A brief introduction to beam position monitoring, 2020.

[4] Alexis Gamelin. Collective effects in a transient microbunching regime and ion cloud mitigation in ThomX. PhD thesis, 09 2018.

[5] Peter Forck. Beam instrumentation and diagnostics, 2020.

[6] Sergey S. Kurennoy. Nonlinearities and effects of transverse beam size in beam position monitors. Phys. Rev. ST Accel. Beams, 4:092801, Sep 2001.